Optimization of Reforming Parameter and Configuration for Hydrogen Production

Zhongxiang Chen and Said S. E. H. Elnashaie
Dept. of Chemical Engineering, Auburn University, Auburn, AL 36849-5127

DOI 10.1002/aic.10406
Published online April 5, 2005 in Wiley InterScience (www.interscience.wiley.com).

In the present investigation optimization is classified into configuration optimization on one hand and optimization of the design and operating parameters for each configuration on the other hand. The process investigated is that of hydrogen production by steam reforming of higher hydrocarbons. Heptane is used as a model component for higher hydrocarbons. The proposed novel reforming process is basically a circulating fluidized-bed membrane reformer (CFBMR) with continuous catalyst regeneration and gas–solid separation. Composite hydrogen-selective membranes are used to remove the product hydrogen from the reacting gas mixture, thus driving the reversible reactions beyond their thermodynamic equilibria. Dense perovskite oxygen-selective membranes are also used to introduce oxygen for the exothermic oxidation of hydrocarbons and carbon. Four configurations are investigated, two of which relate to the catalyst regeneration before the gas–solid separation and the other two related to the catalyst regeneration after the gas–solid separation. The optimization of the performance of each configuration is carried out for a number of design and operating parameters as optimization parameters and under both non-autothermal and autothermal conditions. Results show that the autothermal operation with direct contact between cold feeds (water and heptane) and hot circulating catalyst can be the best configuration for efficient hydrogen production with minimum energy consumption. The maximum net hydrogen yield is 16.732 mol of hydrogen per mol of heptane fed, which is 76.05% of the maximum theoretical hydrogen yield of 22 when the final reforming products are carbon dioxide and hydrogen. Previous investigations never exceeded 70.82% of this theoretical value. © 2005 American Institute of Chemical Engineers *AIChE J,* 51: 1467–1481, 2005
Keywords: circulating fluidized bed, fuel, higher hydrocarbon, hydrogen, membrane reformer, modeling, optimization, steam reforming

Introduction

Hydrogen has been the focus of increased attention as a promising clean fuel for the twenty-first century because it burns to form only water.[1-11] Currently, hydrogen is mainly produced by steam reforming of hydrocarbons, commonly taking place in conventional reforming furnaces that consist of hundreds of parallel fixed-bed catalyst tubes of small diameter to facilitate heat transfer.[12-16] However, fixed-bed steam reformers [first-generation reformers (FGRs)] suffer from a number of important limitations.

(1) *Thermodynamic equilibrium limitation*: The reversibility of the reforming reactions limits the hydrogen production to the thermodynamic equilibrium values.[14,17]

(2) *Diffusion limitation*: The large catalyst particles used in the fixed-bed reformer (such as 16 × 16 × 16-mm Raschig rings[14] and approximately 6- to 17-mm thick-walled rings[17]) make the effectiveness factor of nickel reforming catalyst extremely low, in the range of 0.001–0.01.[14,18-20]

Correspondence concerning this article should be addressed to Z.-X. Chen at this current address: Dept. of Chemical and Biological Engineering, University of British Columbia, 2216 Main Mall, Vancouver, BC, Canada V6T 1Z4; e-mail: chenz@chml.ubc.ca.

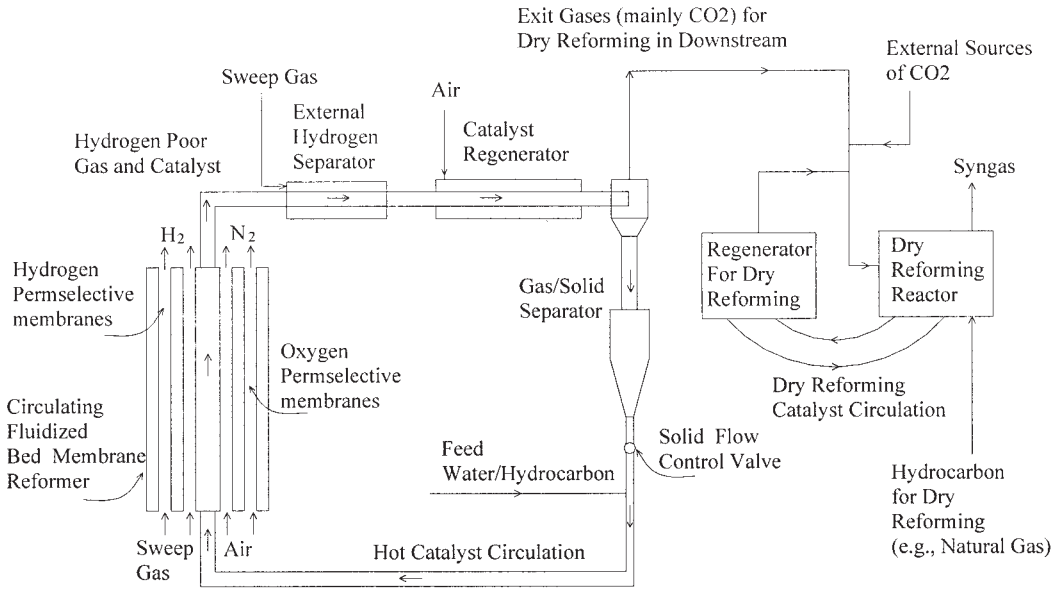

Figure 1. Novel process for efficient hydrogen production by steam reforming of hydrocarbons.

(3) *Carbon formation and catalyst deactivation*: Carbon formation during the steam reforming of hydrocarbons deactivates the catalyst and thus leads to low efficiency, even blocking the reformer.[17,21,22]

(4) *Heat transfer limitation*: Because of the highly endothermic nature of steam reforming reactions, the process is usually operated at high temperatures with a large demand of external heat supply. Only 50% of the heat of combustion is used directly for the steam reforming reactions.[23] Extensive efforts have been devoted to waste heat recovery by generating steam and preheating the feeds.[24]

(5) *Environmental pollutions and CO_2 emission*: More stringent environmental regulations are increasing the control of the emission of pollutions and greenhouse gases during the burning of a number of fuels in huge top-/side-fired furnaces for the heat supply.[25]

Significant progress has been made to overcome the limitations of conventional FGRs in the past few decades. For example, the use of hydrogen-selective membranes "breaks" the thermodynamic equilibrium limitation and enhances the hydrogen production[7,26]; the use of powdered catalyst in a fluidized bed eliminates the diffusion limitation and causes the catalyst effectiveness factor to approach unity[27,28]; the oxidative reforming of hydrocarbons or autothermal reforming of hydrocarbons in the bed supplies the heat for endothermic reforming.[29,30] One of the most successful developments for a more efficient reformer was the bubbling fluidized bed reformer with hydrogen-selective membranes (BFBMR),[27,28,31-34] which can be referred to as the second-generation reformer (SGR). This technology is a proven success for natural gas. Recently, Elnashaie and coworkers proposed a novel process, which consists of a circulating fluidized-bed membrane reformer (CFBMR), and found it to be the more efficient and more flexible process for pure hydrogen production for a wide range of feedstocks such as natural gas, naphtha, higher hydrocarbons, even gasoline, diesel, and bio-oils.[4-11,35]

The CFBMR may be referred to as the third-generation reformer (TGR). As shown in Figure 1, inside this novel CFBMR hydrogen-selective membranes are used to remove the product hydrogen from the reacting gas mixture and therefore drive the reversible reactions beyond their thermodynamic equilibria. Dense perovskite oxygen-selective membranes are used to introduce oxygen from air for the exothermic oxidative reforming of hydrocarbons and carbon oxidation. Between these membrane tubes the nickel reforming catalyst is fast fluidized and steam reforming of higher hydrocarbons takes place. The deactivated catalyst is carried out of the reformer with the exit gas stream, regenerated in a catalyst regenerator, and separated from the gases in a gas–solid separator. Finally, the regenerated hot catalyst is recycled to the riser reformer together with the fresh water and hydrocarbon feeds. To control the emission of CO_2, the gas mixture exit from the gas–solid separator is used as part of the feed to a novel CO_2 dry reformer in the downstream, as shown in the right hand side of Figure 1. The main features of this novel CFBMR are as follows: the use of fine catalyst particles (186 μm) eliminates the severe diffusion limitations in the fixed bed; the use of hydrogen permselective membranes and/or the removal of CO_2 by chemiadsorbent "breaks" the thermodynamic equilibrium limitation; the continuous catalyst regeneration recovers the catalyst activity and provides the possibility for a wide range of feedstocks; the in-site exothermic oxidative reforming of hydrocarbons and the exothermic catalyst regeneration supply the necessary heat for endothermic reforming reactions, making autothermal operation possible, and therefore "breaks" heat transfer limitation. The CO_2 dry reforming of natural gas eliminates the emission of CO_2, making this novel process environmentally benign, and also produces syngas, which can be further converted to valuable fuel additives or chemicals such as methanol.[36,37]

In this paper the optimization of reformer configuration and design/operating parameters for each configuration for the efficient hydrogen production by steam reforming of higher hydrocarbons is performed in the CFBMR part only (without

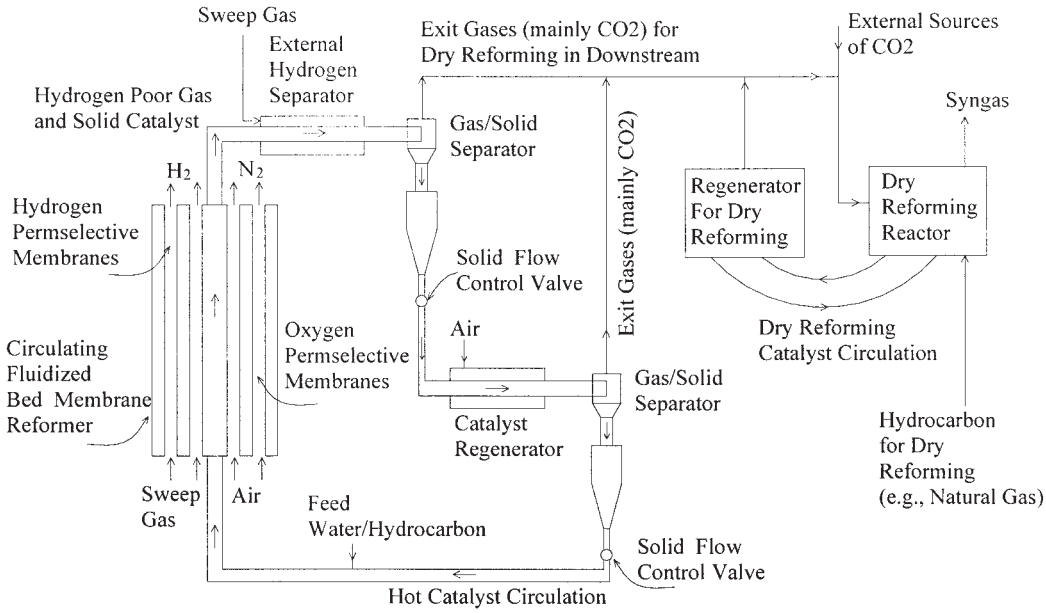

Figure 2. Reformer novel configuration 2: autothermal reforming with catalyst regeneration after gas–solid separation.

the part of CO_2 dry reforming). The objective function for optimization is the net hydrogen yield, given that the cost of raw material hydrocarbon significantly affects the final price of hydrogen.[38] Heptane is used as a model component for higher hydrocarbons (such as diesel, gasoline, bio-oils, etc.). The parameter optimization for the maximum net hydrogen yield is performed under both autothermal and non-autothermal conditions.

Reformer Novel Configurations

Four reformer novel configurations, shown schematically in Figures 1–4, are investigated for the optimization of design/operating parameter and reformer configuration. For the efficient production of hydrogen, the remaining hydrogen exiting from the riser reformer after the hydrogen removal inside the reformer is further removed in an external hydrogen separator for all configurations. For configurations 1 and 3 with catalyst regeneration before the gas–solid separation, the carbon deposited on the nickel reforming catalyst as well as the reformer exit flammable gases such as unreacted heptane and by-products methane and carbon monoxide are burned off by excess air in the catalyst regenerator, whereas for configurations 2 and 4, only the carbon deposited on the nickel reforming catalyst is burned off. Configurations 1 and 2 are autothermally operated

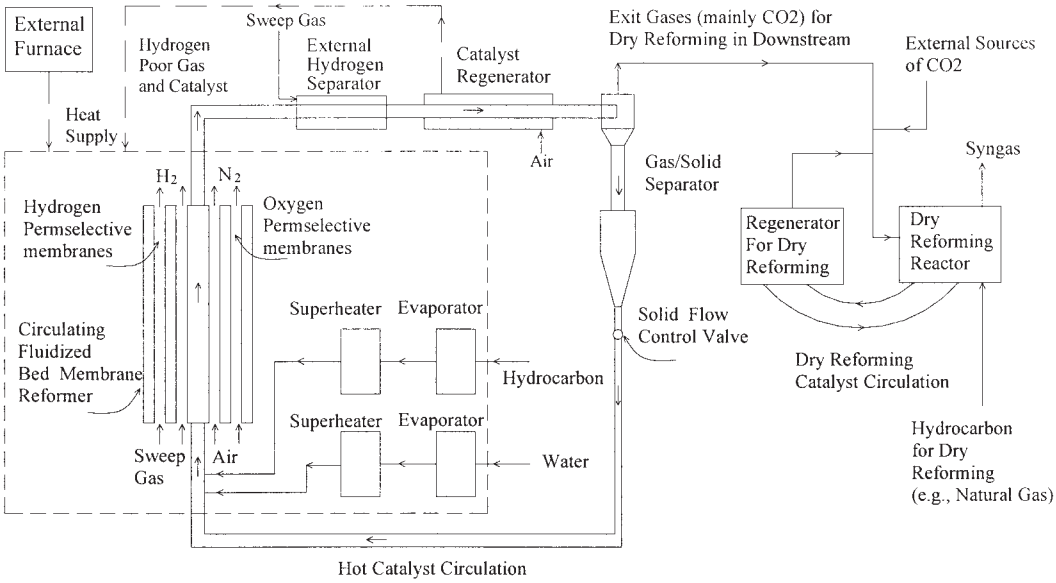

Figure 3. Reformer novel configuration 3: non-autothermal reforming with catalyst regeneration before gas–solid separation.

Dashed line stands for the heat supply in the system.

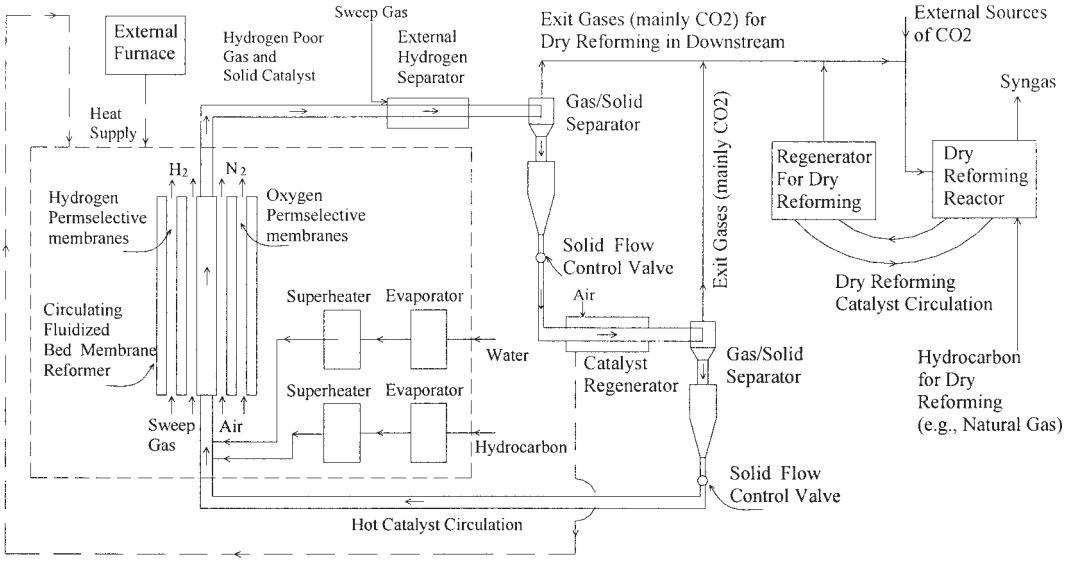

Figure 4. Reformer novel configuration 4: non-autothermal reforming with catalyst regeneration after gas–solid separation.

Dashed line stands for the heat supply in system.

using the heat generated in the catalyst regenerator and the in-site heat of reaction by oxidative reforming of hydrocarbon in the riser reformer. The cold feeds of water and heptane directly contact the hot recycle catalyst before feeding into the riser reformer, whereas configurations 3 and 4 are non-autothermally operated, using the heat generated in both catalyst regenerator and external furnaces as well as the in-site heat of reaction by oxidative reforming of hydrocarbon in the riser reformer. The feeds of cold water and heptane are evaporated in the external evaporators and then superheated to the same temperature as that of the feeding catalyst. The external furnaces are schematically shown by the dashed line/box in Figures 3 and 4, which can be practically arranged to surround the membrane reformer, evaporators, and superheaters to minimize the heat loss. Autothermal reforming is an operation condition such that the heat generated in the adiabatic catalyst regenerator is equal to the heat consumed by endothermic reforming reactions, as well as the heat needed to vaporize and preheat the feeds water and hydrocarbon. This kind of autothermal operation has some resemblance, in principle, to modern fluid catalytic cracking (FCC) units.[39] The main differences among these four configurations are summarized in Table 1.

Reactions and Kinetics

Because oxygen can be introduced into the riser reformer through oxygen-selective membranes, oxidative reforming of heptane and by-product methane takes place simultaneously with endothermic steam reforming. Carbon may be generated by the decompositions of hydrocarbons and carbon monoxide.

Table 1. Main Differences among Four Novel Reformer Configurations

	Operation Mode			
	Autothermal		Non-Autothermal	
Parameter	Configuration 1	Configuration 2	Configuration 1	Configuration 2
Heat sources	In-site oxidative reforming and catalyst regeneration	In-site oxidative reforming and catalyst regeneration	In-site oxidative reforming, catalyst regeneration and external furnace	In-site oxidative reforming, catalyst regeneration and external furnace
Sources for heat generation in catalyst regenerator	Unreacted heptane and methane, carbon monoxide, and deposited carbon	Deposited carbon	Unreacted heptane and methane, carbon monoxide, and deposited carbon	Deposited carbon
External furnace	No	No	Yes	Yes
Contact mode between cold feeds and hot circulating catalyst	Direct	Direct	Indirect after evaporating and superheating	Indirect after evaporating and superheating
Evaporator	No	No	Yes	Yes
Superheater	No	No	Yes	Yes
Location of catalyst regeneration	Before gas–solid separation	After gas–solid separation	Before gas–solid separation	After gas–solid separation
Number of gas–solid separators	1	2	1	2

Table 2. Reactions and Kinetic Rate Equations for the Riser Reformer

Reaction	Reaction Heat (kJ/mol)	Kinetic Rate Equation	Reference
$C_7H_{16} + 7H_2O \rightarrow 7CO + 15H_2$	1108	$r_1 = \dfrac{k_1 P_{C_7H_{16}}}{\left(1 + 25.2\dfrac{P_{C_7H_{16}}P_{H_2}}{P_{H_2O}} + 0.077\dfrac{P_{H_2O}}{P_{H_2}}\right)^2}$	12
$CO + 3H_2 \rightleftharpoons CH_4 + H_2O$	−206.2	$r_2 = k_2\left(\dfrac{P_{CO}P_{H_2}^{0.5}}{K_2} - \dfrac{P_{CH_4}P_{H_2O_2}}{P_{H_2}^{2.5}}\right)\Big/\mathrm{DEN}^2$	13
$CO + H_2O \rightleftharpoons CO_2 + H_2$	−41.2	$r_3 = k_3\left(\dfrac{P_{CO}P_{H_2O_2}}{P_{H_2}} - \dfrac{P_{CO_2}}{K_3}\right)\Big/\mathrm{DEN}^2$	
$CH_4 + 2H_2O \rightleftharpoons CO_2 + 4H_2$	165	$r_4 = k_4\left(\dfrac{P_{CH_4}P_{H_2O_2}^2}{P_{H_2}^{3.5}} - \dfrac{P_{CO_2}P_{H_2}^{0.5}}{K_2K_3}\right)\Big/\mathrm{DEN}^2$	
$C_7H_{16} + 3.5O_2 \rightarrow 7CO + 8H_2$	−961.41	$r_5 = k_5 T P^{0.3} C_{C_7H_{16}}^{0.5} C_{O_2}$	40
$CH_4 + 2O_2 \rightarrow CO_2 + 2H_2O$	−802.562	$r_6 = k_6 P_{CH_4} P_{O_2}$	41
$CH_4 + CO_2 \rightleftharpoons 2CO + 2H_2$	247.05	$r_7 = k_7 P_{CH_4} P_{CO_2}\left(1 - \dfrac{P_{CO}^2 P_{H_2}^2}{K_7 P_{CH_4} P_{CO_2}}\right)$	
$C_7H_{16} \rightarrow 7C + 8H_2$	187.7	$r_8 = k_8 P_{C_7H_{16}}^{0.569}$*	42
$CH_4 \rightleftharpoons C + 2H_2$	74.6	$r_9 = \dfrac{k_9 K_{CH_4}\left(P_{CH_4} - \dfrac{P_{H_2}^2}{K_{9a}}\right)}{\left(1 + \dfrac{P_{H_2}^{1.5}}{K_{9b}} + K_{CH_4}P_{CH_4}\right)^2}$	43
$2CO \rightarrow C + CO_2$	−172.45	$r_{10} = \dfrac{k_{10}P_{CO}}{\left(1 + K_{10a}P_{CO} + K_{10b}\dfrac{P_{CO_2}}{P_{CO}}\right)^2}$	44
$C + H_2O \rightarrow CO + H_2$	131.296	$r_{11} = k_{11} P_{H_2O}^{0.5}$	45
$C + 0.5O_2 \rightarrow CO$	−110.53	$r_{12} = k_{12} P_{O_2}^{0.5}$	
$C + CO_2 \rightarrow 2CO$	172.45	$r_{13} = k_{13} P_{CO_2}^{0.5}$	
		$\mathrm{DEN} = 1 + K_{CO}P_{CO} + K_{H_2}P_{H_2} + K_{CH_4}P_{CH_4} + K_{H_2O}P_{H_2O}/P_{H_2}$	

*Empirically obtained from the experimental data reported by Rostrup-Nielsen.[42]

On the other hand, it may be simultaneously gasified by steam, hydrogen, carbon dioxide, and oxygen. The difference between the carbon formation and gasification is the net carbon deposition on the nickel reforming catalyst. The reactions (referred to as reactions 1–13) and their kinetic rate equations for the riser reformer are summarized in Table 2.

Catalyst regeneration can be carried out before or after the gas–solid separation; accordingly, the reactions in catalyst regenerator are different. For the reformer configurations 1 and 3 with catalyst regeneration before the gas–solid separation, the following four reactions (referred to as reactions 14–17) may take place in the catalyst regenerator

$$C_7H_{16} + 11O_2 \rightarrow 7CO_2 + 8H_2O \quad \Delta H^\circ = -4501.48\ \mathrm{kJ/mol} \tag{1}$$

$$CH_4 + 2O_2 \rightarrow CO_2 + 2H_2O \quad \Delta H^\circ = -802.76\ \mathrm{kJ/mol} \tag{2}$$

$$CO + 0.5O_2 \rightarrow CO_2 \quad \Delta H^\circ = -282.98\ \mathrm{kJ/mol} \tag{3}$$

$$C + O_2 \rightarrow CO_2 \quad \Delta H^\circ = -393.51\ \mathrm{kJ/mol} \tag{4}$$

whereas for the configurations 2 and 4 with the catalyst regeneration after the gas–solid separation, only the burning of carbon (Eq. 4) occurs in the catalyst regenerator.

Process Modeling and Parameter Optimization

Riser reformer modeling

Because of the high gas velocity (~3 m/s) and the use of fine catalyst particles (186 μm) in the circulating fluidized bed, the slip between the gas and solid phases can be negligible.[46] Therefore the CFBMR is modeled as a plug-flow reactor (PFR) with cocurrent flow in membrane sides. The other main assumptions are as follows:

(1) Steady-state operation.

(2) There is no hydrogen oxidation taking place over nickel reforming catalyst. This assumption is based on the experimental result that oxygen can be safely and successfully introduced into a steam reformer, reported by Roy and coworkers.[47]

(3) The palladium-based hydrogen membranes and dense perovskite oxygen membranes are 100% selective for hydrogen and oxygen permeation.[48,49]

(4) The heat capacities of the components and the heat of reactions are constant.

(5) The pressures in the riser reformer and both hydrogen and oxygen membrane tubes are constant.

(6) The hydrogen or oxygen membrane performance is not affected by carbon deposition.

Thus for all above four reforming configurations, the steady-state equations for material balance in the reaction side are given by

$$\frac{dF_i}{dl} = \rho_C(1-\varepsilon)A_f\sum_{j=1}^{13}\sigma_{i,j}r_j - aJ_{H_2}\pi N_{H_2}d_{H_2} + bJ_{O_2}\pi N_{O_2}d_{O_2} \tag{5}$$

where a and b are the control indices for the membrane permeation fluxes. For hydrogen, $a = 1$ and $b = 0$; for oxygen, $a = 0$ and $b = 1$; for all other components, $a = 0$ and $b = 0$. In the reaction side, component i ($i = 1, 2, \ldots, 8$) stands for heptane, methane, carbon dioxide, carbon monoxide, hydrogen, steam, oxygen, and carbon, respectively.

The energy balance equation for the reformer, including the membrane tubes, is given by

$$\frac{dT}{dl} = \frac{\sum_{j=1}^{13} r_j(-\Delta H_j)\rho_C(1-\varepsilon)A_f + \dot{Q}}{\sum_{k=1}^{13} F_k Cp_k} \tag{6}$$

where $\dot{Q}$ is the heating rate along the reactor length (J m^{-1} s^{-1}). Component k ($k = 1, 2, \ldots, 13$) stands for heptane, methane, carbon dioxide, carbon monoxide, hydrogen, steam, oxygen, and carbon in the reaction side, hydrogen and sweep gas in hydrogen-selective membrane tubes, oxygen and nitrogen in oxygen-selective membrane tubes, and the circulating solid catalyst, respectively.

The material balance equation in hydrogen permeation membrane tubes is given by

$$\frac{dF_{H_2,P}}{dl} = \pi N_{H_2}d_{H_2}J_{H_2} \tag{7}$$

The material balance equation in oxygen permeation membrane tubes is given by

$$\frac{dF_{O_2,P}}{dl} = -\pi N_{O_2}d_{O_2}J_{O_2} \tag{8}$$

In this investigation, the hydrogen-selective membrane is assumed to be a porous ceramic tube coated by palladium. For this palladium-based membrane, the hydrogen permeation flux can be calculated using the following equation[48,50]

$$J_{H_2} = \frac{2.003\times10^{-5}}{\delta_{H_2}}\exp\left(\frac{-15{,}700}{RT}\right)\times\left(\sqrt{p_{H_2,r}} - \sqrt{p_{H_2,p}}\right) \quad \text{mol m}^{-2}\,\text{s}^{-1} \tag{9}$$

For a dense perovskite oxygen membrane, the oxygen permeation flux can be calculated using the following equation[49]

$$J_{O_2} = 7.339\times10^{-7}\exp\left(\frac{-62{,}700}{RT}\right)\frac{T}{\delta_{O_2}}\ln\left(\frac{P_{O_2,p}}{P_{O_2,r}}\right) \quad \text{mol m}^{-2}\,\text{s}^{-1} \tag{10}$$

Because the catalyst deactivation occurs when carbon deposits on it, the reaction rate equations are reformulated accordingly by introducing the catalyst activity function as follows

$$r_j = r_{j0}\phi_j \tag{11}$$

where ϕ_j is the specific catalyst activity function for the jth reaction in Table 2 ($j = 1, 2\cdots13$). Chen and coworkers[10] developed an exponential deactivation model equation as follows

$$\phi_j = \begin{cases} \exp(-\alpha_C C_k) & \text{Reaction } j \text{ is affected by carbon deposition} \\ 1.0 & \text{Reaction } j \text{ is not affected by carbon deposition} \end{cases} \tag{12}$$

The value of ϕ_j is calculated by Eq. 12 or equal to 1.0, depending on whether the jth reaction is affected by the catalyst deactivation (that is, whether the jth reaction is a catalytic reaction or a noncatalytic reaction). Herein only the last three reaction rate equations r_{11}, r_{12}, and r_{13} in Table 2 are considered unaffected by the catalyst deactivation because the noncatalytic carbon gasification kinetics are used; r_{j0} is the initial reaction rate with fresh catalyst, given in Table 2.

Heat generation rate in catalyst regenerator

In this investigation the efficiency of catalyst regenerator is considered as a design parameter. We simply assume that the burning of carbon and the combustion of remaining heptane, methane, and carbon monoxide in the catalyst regenerator have the same efficiency. Then the total heat generation rate in the catalyst regenerator for configurations 1 and 3 is

$$Q_g = \sum_{j=14}^{17} F_{j,0}(-\Delta H_j)ER \tag{13}$$

where $F_{j,0}$ ($j = 14\cdots17$) represents the initial molar feeds of remaining heptane, by-products methane, carbon monoxide, and carbon to the catalyst regenerator (in other words, they are equal to the exit molar flow rates of heptane, methane, carbon monoxide, and carbon from the reformer); ΔH_j ($j = 14\cdots17$) represents the heats of reaction for reactions 14 to 17, as

represented by Eqs. 1–4; *ER* is the efficiency of catalyst regenerator.

The total heat generation rate in the catalyst regenerator for configurations 2 and 4 is

$$Q_g = F_{17,0}(-\Delta H_{17})ER \tag{14}$$

Model equations for autothermal reforming

For configurations 1 and 2, the autothermal reforming operation is achieved through the carefully designed coupling between the endothermic riser reformer and exothermic catalyst regenerator. Under the autothermal reforming condition, the total heat generated in the adiabatic catalyst regenerator is equal to the total heat consumed by endothermic reforming reactions, as well as the heat needed to vaporize and preheat the feeds water and hydrocarbon, that is

$$Q_g = Q_C \tag{15}$$

where Q_C is the total process heat consumption rate. Because the riser reformer is operated under an adiabatic condition, the heat necessary for the endothermic reforming reaction inside the reformer is supplied by the superheated steam, heptane, and the hot circulating catalyst. The energy balance for the riser reformer is calculated using Eq. 6. Thus the total heat consumption rate is actually the heat requirement for maintaining the autothermal operation in the system, which can be written as

$$Q_C = \sum_{kk=1}^{2} F_{kk}[(T_{kk,b} - T_{room})Cp_{kk(l)} + \Delta H_{kk,vap} + (T' - T_{kk,b})Cp_{kk,b(g)}] + G_{cat}Cp_{cat}(T' - T_{exit}) \tag{16}$$

Component *kk* ($k = 1, 2$) represents the feeds of water and heptane, respectively.

Under steady-state autothermal operation, the feed temperature T_0 of steam, heptane, and catalyst to the reformer entrance should be equal to the final mixing temperature T' of feeds water, heptane, and recycle catalyst after direct contact, which gives

$$T_0 = T' \tag{17}$$

Model equations for non-autothermal reforming

As shown in Figures 3 and 4, the heats generated both from the catalyst regenerator and the external furnace supply the necessary heat for preheating, evaporating the cold feeds water and heptane, and also for preheating the recycle catalyst and for the endothermic reforming reactions in the riser reformer. Usually during these non-autothermal operations, the heat usage or heat loss is important. Because of the highly endothermic nature of the steam reforming reaction, about 50% of the heat of combustion in the furnace is used directly for the steam reforming reactions.[23] Abundant efforts have been devoted to waste heat recovery by generating steam and preheating the feeds. The process is usually limited by heat transfer and therefore the overall heating efficiency is about 91% after waste heat recovery.[24] In this preliminary investigation, considering the heat transfer limitation for the indirect heating, we introduce a new variable X_{ohe} as the overall external heating efficiency to account for the net heat supply to the riser reformer, evaporators, and superheaters from the external furnace and catalyst regenerator. It is defined as the ratio of how much heat is supplied for the system to the total heat generation in the external furnace and catalyst regenerator. The total heat generation rate (Q_S) is the sum of heat generation rate in the catalyst regenerator (Q_g) and the heat generation rate in the external furnace (Q_f), which is given by

$$Q_S = Q_g + Q_f \tag{18}$$

Then the effective (or net) heat supply rate (Q_{EffS}) for the process is accordingly modified as

$$Q_{EffS} = X_{ohe}(Q_g + Q_f) \tag{19}$$

The effective heat supply for the process is used for the evaporators, superheaters, and riser reformer. The heat consumed in the evaporators and superheaters, including preheating the recycle catalyst, is given by

$$Q_{C1} = \sum_{kk=1}^{2} F_{kk}[(T_{kk,b} - T_{room})Cp_{kk(1)} + \Delta H_{kk,vap} + (T_0 - T_{kk,b})Cp_{kk,b(g)}] + G_{cat}Cp_{cat}(T_0 - T_{exit}) \tag{20}$$

and the heat consumed by heating the riser reformer is

$$Q_{C2} = \int_0^L \dot{Q}\,dl \tag{21}$$

where $\dot{Q}$ is the heating rate along the reactor length, which is defined earlier by Eq. 6.

Thus, we obtain

$$Q_{EffS} = Q_{C1} + Q_{C2} \tag{22}$$

Parameter optimization

The optimization objective, variables, and constraints are defined as follows:

Objective

$(Y_{H_2})_{max}$ Maximum yield of hydrogen

The objective function for optimization is the hydrogen yield, given that the cost of raw material hydrocarbon significantly affects the final price of hydrogen. The reported data show that the feedstock hydrocarbon costs are 52–68% of the total cost for large plants and about 40% for small plants.[38] The yield of hydrogen is defined as the net hydrogen yield, considering the external furnace energy consumption, which can be defined as follows:

Table 3. Design/Operating Parameters and Reaction Conditions for Optimization

Riser Reformer Construction Parameters	
Outside diameter of the reformer tube	0.1154 m [14]
Wall thickness of the riser reformer	0.0088 m [14]
Outside diameter of palladium based hydrogen membrane tubes	0.00489 m [32]
Wall thickness of hydrogen membrane tubes	0.00024 m [32]
Thickness of palladium layer on hydrogen membranes tubes	20 μm [48]
Outside diameter of oxygen membranes tubes	0.00489 m
Thickness of dense perovskite film on oxygen membrane tubes	50 μm[52]
Nickel Steam Reforming Catalyst	
Catalyst particle density	2835 kg/m^3 [14]
Mean diameter of catalyst particles	186 μm [32]
Operating Conditions in Membrane Tubes	
Operating pressure in palladium based hydrogen membrane tubes	101.3 kPa
Operating pressure in oxygen membrane tubes	3039 kPa

$$Y_{H_2} = \frac{\text{Total hydrogen produced} - \text{Equivalent hydrogen consumed for same heat generation in furnace}}{\text{Process heptane feed}} \tag{23}$$

Variables

- T_0 feed temperature to the riser reformer (it is a variable for non-autothermal reforming only because for the autothermal reforming it is automatically determined by the configuration)
- N_{H_2} number of hydrogen membrane tubes
- N_{O_2} number of oxygen membrane tubes
- S/C steam to carbon (of heptane) feed ratio
- P reaction pressure
- L reactor length
- GFR total feed gas flow rate
- SF solid fraction in the CFB bed
- ER efficiency of catalyst regenerator
- $\dot{Q}$ effective heating rate to riser reformer (it is a variable for non-autothermal reforming only, given that for autothermal reforming it is actually zero)

Constraints

(1) To leave enough space between the membrane tubes for the fine catalyst particles to circulate freely in the CFBMR, in practice the membrane tubes must be separated by a distance of at least 20 to 30 times the diameter of the catalyst particles.[51] According to the dimensions of the reformer and the membrane tubes shown later in Table 3, the maximum number of membrane tubes is 109 using triangle arrangement. Therefore,

$$N_{H_2} + N_{O_2} \le 109 \qquad N_{H_2} \ge 0 \qquad N_{O_2} \ge 0 \tag{24}$$

(2) To avoid hot spots or "runaway" in the CFBMR, and also to avoid extinction of the reforming, the range of the reactor operating temperature is roughly set as

$$500 \le T \le 1150 \text{ K} \tag{25}$$

(3) Typically the industrial steam reformer is operated under 1–30 atm; thus the range of operating pressure is set as

$$1 \le P \le 30 \tag{26}$$

(4) The range of reactor length is chosen as

$$0 < L \le 2 \tag{27}$$

(5) During the parameter optimization, the CFBMR is always checked and verified to be simulated under the circulating fluidized regime using the method reported by Kunii and Levenspiel.[53,54] Accordingly, the total feed gas flow rate is in the range of

$$2.41 \text{ kmol} \le GFR \le 28.92 \text{ kmol/h} \tag{28}$$

(6) In a typical CFB reactor, the solid fraction varies in a range of 0.01 to 0.22 v/v[53,54]; then

$$0.01 \le SF \le 0.22 \tag{29}$$

(7) The range of efficiency of catalyst regenerator ER is given by

$$0 < ER \le 1 \tag{30}$$

Under autothermal operation, the feed temperature to the riser reformer T_0 is a system variable rather than a feed parameter, and the net heat supply rate to the riser reformer $\dot{Q}$ is zero. Therefore, the parameter optimization for both autothermal and non-autothermal reforming can be summarized as follows:

Objective

$$(Y_{H_2})_{max} = \begin{cases} f(N_{H_2}, N_{O_2}, S/C, P, L, GFR, SF, ER) \\ \quad \text{Autothermal reforming} \\ f(T_0, N_{H_2}, N_{O_2}, S/C, P, L, GFR, SF, ER, \dot{Q}) \\ \quad \text{Non-autothermal reforming} \end{cases} \tag{31}$$

subject to

$$\begin{cases} N_{H_2} + N_{O_2} \le 109 \qquad N_{H_2} \ge 0 \quad N_{O_2} \ge 0 \\ 500 \le T, T_0 \le 1150 \text{ K} \\ 1 \le P \le 30 \\ 0 < L \le 2 \\ 2.41 \le GFR \le 28.92 \\ 0.01 \le SF \le 0.22 \\ 0 < ER \le 1 \end{cases} \tag{32}$$

The optimization problem is solved using the flexible tolerance optimization method (FTOM),[55] with the other design/operating parameters and reaction conditions given in Table 3.

Results and Discussion

Process analysis for autothermal and non-autothermal reforming

First we carry out some process calculations to show the importance of the suggested autothermal reforming. Because product hydrogen is continuously removed from the reaction side using selective membranes, the reversible reactions for steam reforming of heptane may be simply represented by the following reaction with final products of carbon dioxide and hydrogen

$$C_7H_{16} + 14H_2O \rightarrow 7CO_2 + 22H_2 \qquad \Delta H^\circ = 819.6 \text{ kJ/mol} \tag{33}$$

In the reformer, carbon can be formed by the heptane cracking, methane cracking, and carbon monoxide decomposition. However, the most important reaction for carbon formation is the heptane cracking, which is given in Table 2 as follows

$$C_7H_{16} \rightarrow 7C + 8H_2 \qquad \Delta H^\circ = 187.7 \tag{34}$$

In the catalyst regenerator, the deposited carbon on the catalyst is burned off using air, which is represented by the following reaction

$$C + O_2 \rightarrow CO_2 \qquad \Delta H^\circ = -393.51 \text{ kJ/mol} \tag{4}$$

Under autothermal reforming, we assume x fraction of 1 mol/s heptane fed is used for steam reforming according to Eq. 33, and $(1 - x)$ fraction of 1 mol/s heptane fed is used for heptane cracking. Thus the amount of carbon formed is $7(1 - x)$ and the total heat generation rate in the catalyst regenerator by burning the carbon is

$$7 \times 393.51 \times (1 - x) \tag{35}$$

If the process heat is mainly consumed for the endothermic reactions (Eqs. 34 and 4), and for the vaporization of feeds water and heptane, then the total heat consumption is given by

$$819.6x + 187.7(1 - x) + 14x \times 40.656 + [x + (1 - x)] \times 31.69 \tag{36}$$

For the autothermal reforming configurations 1 and 2, given that the feeds water and heptane directly contact the hot recycle catalyst, we assume there are no heat losses. Then for autothermal reforming, the total heat generation is equal to the total heat consumption

$$7 \times 393.51 \times (1 - x) = 819.6x + 187.7(1 - x) + 14x \times 40.656 + [x + (1 - x)] \times 31.69 \tag{37}$$

Then the calculated value of x from Eq. 37 is 0.6409. The net hydrogen yield is given by

$$Y_{H_2} = \frac{22x + 8(1 - x)}{1 \text{ mol heptane fed}} = 16.973 \text{ (mol of hydrogen per mol of heptane fed)} \tag{38}$$

We can also get the steam to carbon feed ratio for the above autothermal process

$$S/C = \frac{14x}{1 \times 7} = 2x = 1.282 \qquad \text{mol/mol} \tag{39}$$

For the non-autothermal reforming configurations 3 and 4, the feeds water and heptane do not directly contact the hot recycle catalyst; that is, we assume there are heat transfer limitation and heat losses in the process. Similarly, we assume x fraction of 1 mol/s heptane fed is used for steam reforming according to Eq. 33 and $(1 - x)$ fraction of 1 mol/s heptane fed is used for heptane cracking. As mentioned earlier under process modeling and parameter optimization, we have introduced the overall external heating efficiency X_{ohe} for effective heat supply from the catalyst regeneration and external furnace; then for non-autothermal reforming, the total effective heat supply (from the catalyst regenerator and external furnace) is equal to the total heat consumption in the process

$$[7 \times 393.51 \times (1 - x) + Q_f]X_{ohe} = 819.6x + 187.7(1 - x) + 14x \times 40.656 + [x + (1 - x)] \times 31.69 \tag{40}$$

or

$$x = \frac{2754.57X_{ohe} + Q_fX_{ohe} - 219.39}{1201.084 + 2754.57X_{ohe}} \tag{41}$$

Then the net hydrogen yield defined by Eq. 23 is

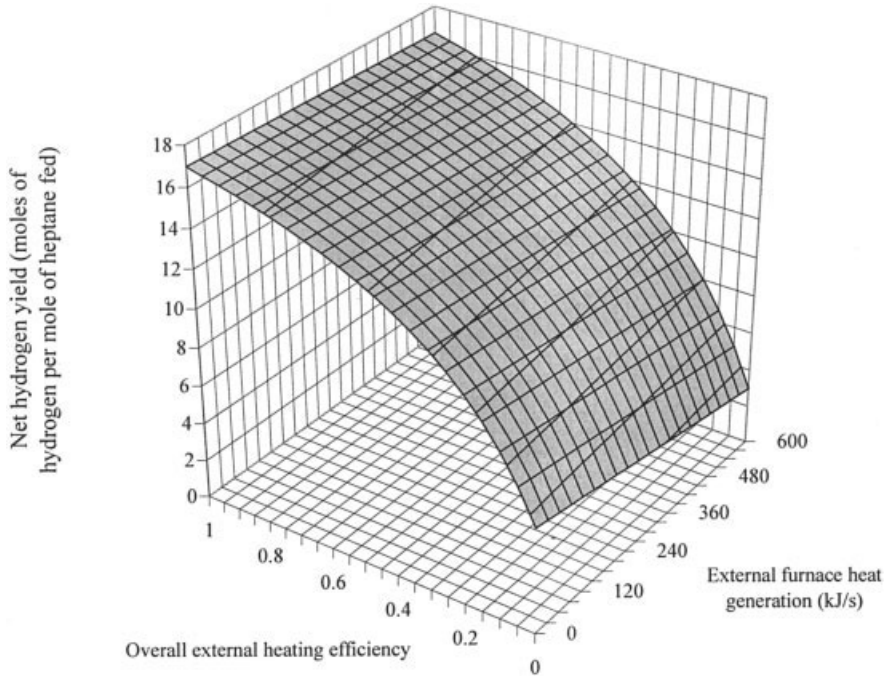

Figure 5. Calculated net hydrogen yield as a function of overall external heating efficiency and external furnace heat generation for non-autothermal processes.

$$Y_{H_2} = \frac{22x + 8(1-x) - \dfrac{Q_f}{[-\Delta H_{f(H_2O)}]}}{1 \text{ mol heptane fed}} = 8 + 14 \times \frac{2754.57X_{ohe} + Q_f X_{ohe} - 219.39}{1201.084 + 2754.57X_{ohe}} - \frac{Q_f}{241.826} \quad (42)$$

and the steam-to-carbon feed ratio for non-autothermal reforming is given by

$$S/C = \frac{14x}{1 \times 7} = 2x = 2 \times \frac{2754.57X_{ohe} + Q_f X_{ohe} - 219.39}{1201.084 + 2754.57X_{ohe}} \quad \text{mol/mol} \quad (43)$$

Therefore for non-autothermal reforming, the net hydrogen yield and operating steam to carbon feed ratio are functions of the condition of non-autothermal processes, that is, the overall external heating efficiency X_{ohe} and the heat generation rate in the external furnace Q_f.

Figures 5 and 6 show the net hydrogen yield and operating steam-to-carbon feed ratio for non-autothermal processes as functions of overall external heating efficiency and external furnace heat generation rate. Generally, the calculated net hydrogen yield and the operating steam-to-carbon feed ratio increase with the increase of overall external heating efficiency for non-autothermal reforming operations. The calculated net hydrogen yield decreases with increasing external furnace heat generation, whereas the operating steam to carbon feed ratio increases with increasing external furnace heat generation. In fact, when the overall external heating efficiency is unity and the external furnace heat generation is zero, the reformer performance under non-autothermal condition is exactly the same as that under autothermal condition, in which cold feeds water and heptane directly contact the hot circulating catalyst. Therefore it is clearly shown in Figure 5 that the autothermal reformer configuration with direct contact between the feeds and hot circulating catalyst (which is equivalent to the non-autothermal reforming with zero external furnace heat generation rate and unity overall external heating efficiency) provides the maximum net hydrogen yield because of the efficient use of heat in the whole process.

Parameter optimization and reformer performance

Table 4 shows the optimization results for the four reforming configurations considered in this investigation. Note that for configurations 3 and 4 (non-autothermal operations) the results are obtained with the values of overall external heating efficiencies of 50 and 100%, respectively. For both autothermal and non-autothermal operations, the configuration with catalyst regeneration before the gas–solid separation (that is, configuration 1 or 3) has higher optimal net hydrogen yield than that of the configuration with catalyst regeneration after the gas–solid separation (that is, configuration 2 or 4). This phenomenon can be explained as follows: For configurations 1 and 3, heat generation in the catalyst regenerator is from the burning of the deposited carbon on the catalyst and the combustion of unreacted hydrocarbons (heptane and methane) and carbon monoxide, whereas for configurations 2 and 4, heat generation in the catalyst regenerator is from the burning of the deposited carbon on the catalyst only.

On the other hand, the optimal effective (net) heating rates to the riser reformer for the non-autothermal operations (configurations 3 and 4) in Table 4 are small. For the autothermal reforming (configurations 1 and 2), the external heating rate is

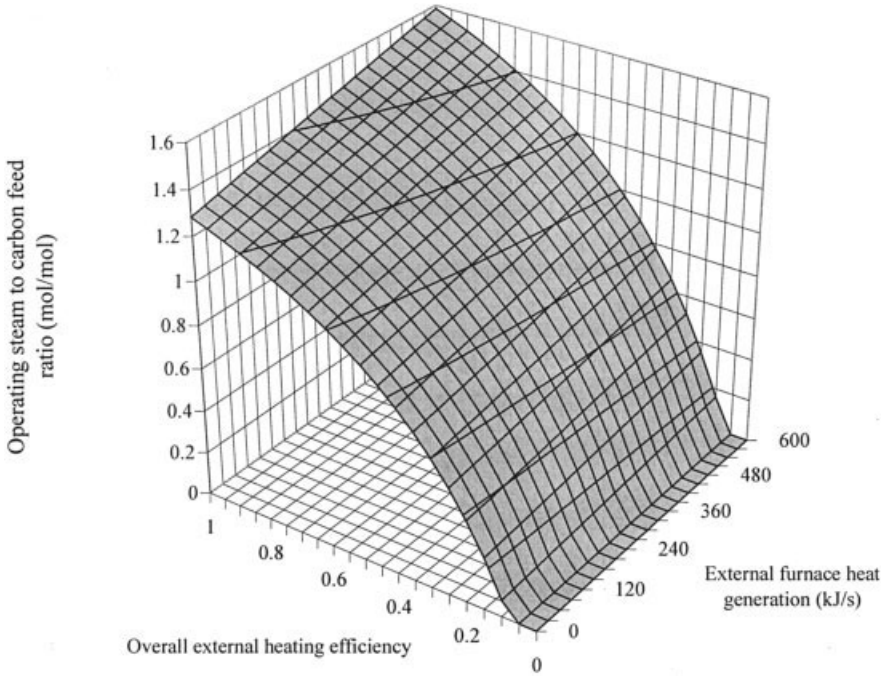

Figure 6. Calculated optimal steam to carbon feed ratio as a function of overall external heating efficiency and external furnace heat generation for non-autothermal processes.

zero. Therefore, for configurations 2 and 4 heat generation rates in the catalyst regenerator must be high enough to maintain the steady-state operation. The only way to achieve that is to operate at higher temperatures and/or lower steam-to-carbon feed ratios to form sufficient carbon for generating enough heat in the catalyst regenerator. Because steam reforming not only extracts hydrogen from hydrocarbon, but also extracts hydrogen from water (whereas carbon formation from hydrocarbon cracking extracts hydrogen only from hydrocarbon), the higher the formation of carbon, the lower the hydrogen production. As

Table 4. Parameter Optimization Results for Configurations 1–4

	Autothermal Reforming		Non-Autothermal Reforming			
			Configuration 3		Configuration 4	
Parameter	Configuration 1	Configuration 2	50%*	100%*	50%*	100%*
Feed temperature (K)	NA**	NA**	826.912	839.185	998.765	857.696
Number of hydrogen membrane tubes†	16.471	39.085	12.244	16.472	19.817	39.085
Number of oxygen membrane tubes†	71.842	69.640	70.787	71.843	80.576	69.641
Steam-to-carbon feed ratio (mol/mol)	1.325	1.431	0.793	1.316	0.653	1.433
Reaction pressure (kPa)	29.811	6.634	22.083	29.811	12.074	6.626
Reactor length (m)	1.731	1.852	1.402	1.731	2.00	1.853
Total feed gas flow rate (kmol/h)	2.517	2.410	2.488	2.518	9.712	2.412
Solid fraction in bed (v/v)	0.0187	0.0131	0.220	0.0196	0.162	0.0167
Efficiency of catalyst regenerator	1.00	1.00	1.00	1.00	1.00	1.00
Effective heating rate to riser reformer (J/s)	NA	NA	−21.451	−26.657	0.813	−20.266
Heat generation rate in external furnace (J/s)	NA	NA	344.723	1.922	1559.5	190.35
Hydrogen production per unit volume of reformer (kg h^{-1} m^{-3})	630.40	492.33	931.58	634.39	2808.44	491.41
Optimal net hydrogen yield (mol of hydrogen per mol of heptane fed)	16.732	15.656	12.917	16.728	12.102	15.642

* The percentage is the overall external heating efficiency for non-autothermal reforming.
**NA = not applicable.
† For practical applications, the number of membranes should be the closet nonfraction values.

a result, configuration 1 (or 3) has a higher optimal net hydrogen yield than that of configuration 2 (or 4). For example, for autothermal operation, the optimal net hydrogen yield is 16.732 mol of hydrogen per mol of heptane fed for configuration 1, whereas it is 15.656 for configuration 2. The improvement of optimal net hydrogen yield for the autothermal configuration 1 is 6.87% compared to that of the autothermal configuration 2. For the non-autothermal configuration 3, the optimal net hydrogen yields are 12.917 and 16.728 for the cases with 50 and 100% overall external heating efficiency, respectively, whereas for the non-autothermal configuration 4, the optimal net hydrogen yields are 12.102 and 15.642 for both cases with 50 and 100% overall external heating efficiency. The improvements are 6.73 and 6.94%, respectively.

Table 4 shows that the efficiency of catalyst regeneration is always 100% for the optimum results, which implies that for the best reformer performance, the use of heat generated from the catalyst regeneration is very important because it decreases the requirement of heat supply from external furnace, making the process both an efficient hydrogen producer and energy saving. For practical applications, the catalyst regenerator can be overdesigned and/or using high air feed. As shown in Table 4, although the effective heating rate to riser reformer for optimized configurations 3 and 4 may be negative, it does not mean that we need to remove the heat from the reactor because the values of these negative heating rates are so small compared to the endothermic heat requirement for the process. For example, for the non-autothermal reforming configuration 3 with 50% overall heating efficiency, the heat requirement for preheating the cold feeds water to generate steam, heptane, and recycle catalyst is 91,254 J/s, whereas the required effective heating rate to the riser reformer is only -21.451 J/s, which is about -0.024% of the entire heat requirement. In fact, the hot feeds steam and heptane, and also the hot circulating catalyst (especially the latter), carry the heat needed for the endothermic reforming reactions inside the reformer. Because of the large mass flow ratio of solid catalyst to the gas stream in the reformer, one of the important roles of the circulating solid catalyst in the circulating fluidized bed is as a heat carrier for the endothermic reforming reactions. For practical applications, the small negative effective heating rates to the riser reformer can be considered as "zero" external heating.

Table 4 also shows that the optimal heat generation rates in external furnaces for the non-autothermal reforming configurations 3 and 4 are very small, which implies that the necessary heat for the endothermic steam reforming is mainly supplied from the catalyst regeneration. The small optimum heat generation rates in external furnace and small negative effective heating rates to the riser reformer both imply that the use of external furnaces will significantly affect the hydrogen production. As defined by Eq. 23, the greater the external heat use, the lesser the net hydrogen yield. Lower net hydrogen yield is the penalty for using external heat for non-autothermal operations, especially when the overall external heating efficiency is low (or there is a large heat loss). For example, for non-autothermal configurations 3 and 4, the optimal net hydrogen yields are 12.917 and 12.102 for 50% overall external heating efficiency, and 16.728 and 15.642 for 100% overall external heating efficiency. The improvements of the optimal net hydrogen yields, arising from the higher overall external heating efficiencies, are 29.50 and 29.25%, respectively.

Table 4 further shows that for the non-autothermal configurations 3 and 4 with 50% overall external heating efficiency, the solid fractions are an order of magnitude greater than those of the other configurations. This phenomenon is explained by the significant heat loss for those cases with low heating efficiency of 50%. Because the optimum external heating rates from the furnaces are negligible, producing the necessary heat for endothermic reforming is mainly supplied by the catalyst regenerator. Because 50% overall external heating efficiency supplies less heat than that of 100% efficiency, the larger catalyst solid fraction carries more heat and somewhat addresses the problem of low heating. In addition, because of the high nonlinear relationship between overall heating efficiency and process performance, the solid fraction for 50% efficiency cases is much larger than that of the other cases.

For the non-autothermal operations with 100% overall external heating efficiency, the reformer performance is almost identical to that of the autothermal operations. For example, for non-autothermal configurations 3 and 4 with 100% overall heating efficiency the optimal net hydrogen yields are 16.728 and 15.642, and for the autothermal configurations 1 and 2 the optimal net hydrogen yields are 16.732 and 15.656, respectively. This is attributed to the fact that when the overall heating efficiency is 100%, there is no heat loss. As mentioned earlier, the external heat generation rates in furnaces are rather small or negligible for these optimum non-autothermal configurations 3 and 4. As a result, the reformer performance under the non-autothermal condition should be very similar to the autothermal cases (no heat loss during the direct contact between the hot recycle catalyst and cold feeds in the adiabatic system). However, for the non-autothermal reforming with external furnaces, the assumption of 100% overall heating efficiency is highly unrealistic because practical application is accompanied with significant heat loss. Armor[23] reported that about 50% of the heat of combustion in the furnace is used directly for the steam reforming reactions. Tindall and King[24] reported that the overall reformer efficiency for fixed-bed steam reformers is about 91% after waste heat recovery. Considering the possible waste heat recovery in practical applications, the overall heating efficiency should be in the range of 50–91%. For the non-autothermal reforming configurations 3 and 4, the reformer performance is simulated and optimized within the range of 50–91% overall heating efficiency.

Figure 7 shows the optimum net hydrogen yield as a function of overall external heating efficiency. The horizontal lines in Figure 7 show the corresponding optimum net hydrogen yields for the autothermal configurations 1 and 2, which are considered as not affected by the overall external heating efficiency. For the non-autothermal configurations 3 and 4, the optimum net hydrogen yield increases with increasing overall heating efficiency. For example, for the non-autothermal reforming configuration 3, the optimal net hydrogen yields are 12.917 and 16.360 mol of hydrogen per mol of heptane fed for the overall heating efficiencies of 50 and 91%, and for the non-autothermal reforming configuration 4, the optimal net hydrogen yields are 12.102 and 15.266, respectively. Because the practical overall heating efficiency is in a range of 50–91% for indirect heating system, the optimum net hydrogen yields are in the range of 12.917–16.360 for non-autothermal configuration 3 and 12.102–15.266 for non-autothermal configuration 4, whereas for the autothermal configurations 1 and 2, the optimal

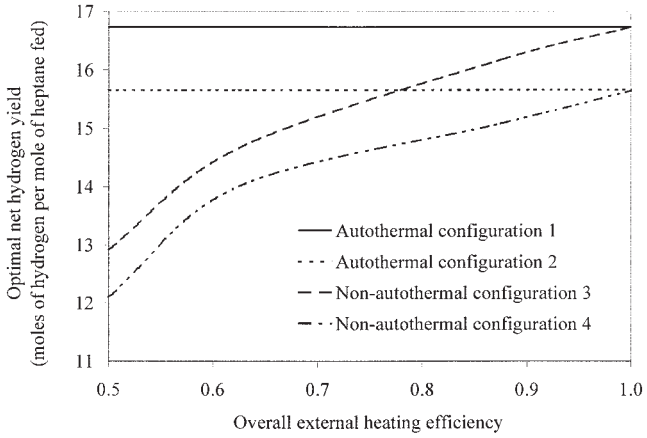

Figure 7. Optimal net hydrogen yield as a function of overall external heating efficiency.

net hydrogen yields are 16.732 and 15.656, respectively. Therefore the improvements of optimal net hydrogen yield using direct contact autothermal reforming are in the range of 2.27–29.53% for configuration 1 compared with configuration 3, and 2.55–29.37% for configuration 2 compared with configuration 4, respectively.

The results show that the autothermal configuration 1 is the best reformer configuration for efficient hydrogen production with minimum energy consumption. The maximum net hydrogen yield is 16.732 mol of hydrogen per mol of heptane fed, which is about 76.05% of the maximum theoretical hydrogen yield of 22 when the final reforming products are carbon dioxide and hydrogen for steam reforming of heptane. Before this optimization investigation, the reported net hydrogen yield is 15.58, which is 70.82% of the theoretical maximum.[11] Thus through this optimization of process parameter and reformer configuration the optimum process performance is obtained.

Conclusions

Optimization of reformer configuration and process design/operating parameter for each of the four configurations considered has been performed for efficient hydrogen production by steam reforming of higher hydrocarbons. Heptane is used as a model component for higher hydrocarbons. The novel reforming process is basically a circulating fluidized-bed membrane reformer (CFBMR) with continuous catalyst regeneration and gas–solid separation. The optimization of the performance of each configuration is carried out for a number of design and operating parameters as optimization parameters and under both non-autothermal and autothermal conditions. For autothermal operations, the cold feeds water and heptane directly contact the hot circulating catalyst, whereas for the non-autothermal operations, the colds feeds water and heptane do not directly contact the hot catalyst.

Four different reforming configurations are investigated, two of which relate to the catalyst regeneration before the gas–solid separation and the other two related to the catalyst regeneration after the gas–solid separation. Results show that the net hydrogen yield for non-autothermal operations increases with increasing process overall external heating efficiency. The use of an external furnace for heat supply to the endothermic reforming process decreases the net hydrogen yield because of the heat losses and heat transfer limitation associated with the external heating methods. The first autothermal reforming configuration with catalyst regeneration before the gas–solid separation is the best configuration for the efficient hydrogen production with minimum energy consumption. The maximum net hydrogen yield is 16.732 mol of hydrogen per mol of heptane fed, which is 76.05% of the maximum theoretical hydrogen yield of 22. Previous investigations never exceeded 70.82% of this theoretical value.[11]

Notation

a, b = control indices for the membranes fluxes of hydrogen and oxygen components
A_f = free cross-sectional area of the reactor, m^2
C_i = molar concentration of component i, mol/m^3
C_k = concentration of deposited coke on the catalyst, g/g catalyst
Cp_{cat} = specific heat of solid catalyst, J g catalyst^{-1} K^{-1}
Cp_i = specific heat of component i, J mol^{-1} K^{-1}
d_i = outside diameter of hydrogen or oxygen-selective membrane tubes ($i = H_2$ or O_2), m
DEN = DEN term, given in the Table 2
ER = efficiency of catalyst regenerator
F_i = molar flow rate of component i ($i = 1, 2, \ldots, 13$), mol/s
F_j = initial molar flow rate of component j ($j = 14 \cdots 17$, stands for unreacted heptane, methane, carbon monoxide, and carbon exiting from reformer) to catalyst regenerator, mol/s
G_{cat} = mass flow rate of catalyst, g/s
GFR = total feed gas flow rate, kmol/h
ΔH° = enthalpy change, J/mol
$\Delta H_{f(H_2O)}$ = enthalpy change of formation of water, J/mol
ΔH_j = heat of reaction for the jth reaction, J/mol
ΔH_{vap} = heat of vaporization, J/mol
J_i = permeation flux of hydrogen or oxygen ($i = H_2$ or O_2), mol m^{-2} s^{-1}
k_j = generalized (forward) reaction rate constant for the jth (reversible) reaction
K_i = absorption constants of component i
K_j = reaction equilibrium constant of the jth reaction
l = length of reactor, m
L = total reactor length, m
N_i = number of hydrogen or oxygen-selective membrane tubes ($i = H_2$ or O_2)
P = reaction pressure, kPa
P_i = partial pressure of component i, kPa
$\dot{Q}$ = heating rate along the reactor length, J s^{-1} m^{-1}
Q_C = total heat consumption rate, J/s
Q_{C1} = heat consumption rate for evaporating and superheating the feeds water and heptane, J/s
Q_{C2} = heating rate to the riser reformer for non-autothermal reforming configurations, J/s
Q_{EffS} = effective heat supply rate to the process, J/s
Q_f = heat generation rate in external furnace, J/s
Q_g = heat generation rate in catalyst regenerator, J/s
Q_S = total heat generation rate in catalyst regeneration and external furnace, J/s
r_j = generalized reaction rates, mol g catalyst^{-1} s^{-1}
r_j = generalized reaction rates with fresh catalyst, mol g catalyst^{-1} s^{-1}
R = gas constant, 8.314 J mol^{-1} K^{-1}
S/C = steam-to-carbon (of heptane) feed ratio, mol/mol
SF = solid fraction in the bed, v/v
T = temperature, K
T_{exit} = riser reformer exit temperature, K
$T_{kk,b}$ = boiling temperature of component kk, K
T = feed temperature to the riser reformer, K
T' = mixing temperature of steam, heptane, and recycled hot catalyst, K
T_{room} = room temperature, K

x = fraction of 1 mol/s of heptane fed for steam reforming with final products of carbon dioxide and hydrogen for process analysis
X_{ohe} = overall external heating efficiency
Y_{H_2} = net hydrogen yield

Greek letters

α_C = deactivation constant, g catalyst/g coke
δ_i = thickness of hydrogen or oxygen membranes ($i = H_2$ or O_2), m
ε = void fraction
π = 3.1415926
ρ_c = density of catalyst, kg/m^3
$\sigma_{i,j}$ = stoichiometric coefficient of component i for the jth reaction
ϕ = catalyst activity function

Subscripts

max = maximum net hydrogen yield
p = hydrogen or oxygen permeation membrane side
r = reaction side in the riser reformer

Literature Cited

1. Dülger Z, Özçelik KR. Fuel economy improvement by on board electrolytic hydrogen production. *Int J Hydrogen Energy*. 2000;25: 895-897.
2. Pehr K, Sauermann P, Traeger O, Bracha M. Liquid hydrogen for motor vehicles—The world's first public LH_2 filling station. *Int J Hydrogen Energy*. 2001;26:777-782.
3. Goltsov VA, Nejat Veziroglu T. A step on the road to hydrogen civilization. *Int J Hydrogen Energy*. 2002;27:719-723.
4. Chen Z, Elnashaie SSEH. Efficient production of hydrogen from higher hydrocarbons using novel membrane reformer. Proc. of the 14th World Hydrogen Energy Conference, Montreal, Canada; 2002.
5. Chen Z, Elnashaie SSEH. Bifurcation behavior and the efficient pure hydrogen production for fuel cells using novel autothermic membrane circulating fluidized bed (CFB) reformer. *Ind Eng Chem Res*. 2004; 43(18):5449-5459.
6. Chen Z, Yan Y, Elnashaie SSEH. Using coking and decoking model in a circulating fast fluidized bed membrane reformer for efficient production of pure hydrogen by steam reforming of higher hydrocarbons. Proc. of the Regional Symposium on Chemical Engineering and the 16th Symposium of Malaysian Chemical Engineers, Kuala Lumpur, Malaysia, 2002:1239-1247.
7. Chen Z, Yan Y, Elnashaie SSEH. Modeling and optimization of a novel membrane reformer for higher hydrocarbons. *AIChE J*. 2003; 49:1250-1265.
8. Chen Z, Yan Y, Elnashaie SSEH. Novel circulating fast fluidized bed membrane reformer for efficient production of hydrogen from steam reforming of methane. *Chem Eng Sci*. 2003;58:4335-4349.
9. Chen Z, Yan Y, Elnashaie SSEH. Hydrogen production and carbon formation during the steam reforming of heptane in a novel circulating fluidized bed membrane reformer. *Ind Eng Chem Res*. 2004;43:1323-1333.
10. Chen Z, Yan Y, Elnashaie SSEH. Catalyst deactivation and engineering control for steam reforming of higher hydrocarbons in a novel membrane reformer. *Chem Eng Sci*. 2004;59(10):1965-1978.
11. Chen Z, Elnashaie SSEH. Steady-state modeling and bifurcation behavior of circulating fluidized bed membrane reformer–regenerator for the production of hydrogen for fuel cells from heptane. *Chem Eng Sci*. 2004;59:3965-3979.
12. Tottrup PB. Evaluation of intrinsic steam reforming kinetic parameters from rate measurements on full particle size. *Appl Catal*. 1982;4:377-389.
13. Xu J, Froment GF. Methane steam reforming, methanation and water–gas shift: I. Intrinsic kinetics. *AIChE J*. 1989;35:88-96.
14. Elnashaie SSEH, Elshishini SS. *Modelling, Simulation and Optimization of Industrial Fixed Bed Catalytic Reactors*. London, UK: Gordon & Breach Science Publishers; 1993.
15. Scholz WH. Processes for industrial production of hydrogen and associated environmental effects. *Gas Sep Purif*. 1993;7:131-139.
16. Christensen TS. Adiabatic prereforming of hydrocarbons—An important step in syngas production. *Appl Catal A: Gen*. 1996;138:285-309.
17. Twigg MV. *Catalyst Handbook*. 2nd ed. London, UK: Wolfe Publishing; 1989:225-282.
18. Rostrup-Nielsen J. Hydrogen via steam reforming of naphtha. *Chem Eng Prog*. 1977;9:87.
19. De Deken JC, Devos EF, Froment GF. Steam reforming of natural gas. *Chem React Eng ACS Symp Ser*. 1982:196.
20. Soliman MA, Elnashaie SSEH, Al-Ubaid AS, Adris AM. Simulation of steam reforming for methane. *Chem Eng Sci*. 1988;43:1801-1806.
21. Bartholomew CH. Mechanisms of catalyst deactivation. *Appl Catal A: Gen*. 2001;212:17-60.
22. Ren X-H, Bertmer M, Stapf S, Demco DE, Blumich B, Kern C, Jess A. Deactivation and regeneration of a naphtha reforming catalyst. *Appl Catal A: Gen*. 2002;228:39-52.
23. Armor JN. Review: The multiple roles for catalysis in the production of H_2. *Appl Catal A: Gen*. 1999;176:159-176.
24. Tindall BM, King DL. Designing steam reformers for hydrogen production. *Hydrocarb Process*. 1994;July:69-75.
25. Intergovernmental Panel on Climate Change (IPCC). *Third Assessment Report of the IPCC: Summary for Policy-Makers*. Geneva, Switzerland: IPCC; 2001.
26. Sammels AF, Schwartz M, Mackay RA, Barton TF, Peterson DR. Catalytic membrane reactors for spontaneous synthesis gas production. *Catal Today*. 2000;56:325.
27. Elnashaie SSEH, Adris AM. A fluidized bed steam reformer for methane. In: Grace J, Shemilt LW, Bergougnou MM, eds. *Proceedings of the VI International Fluidization Conference*. Banff, Canada: AIChE Publication; 1989:319.
28. Adris AM, Elnashaie SSEH, Hughes R. A fluidized bed membrane reactor for the steam reforming of methane. *Can J Chem Eng*. 1991; 69:1061.
29. Hayakawa T, Andersen AG, Shimizu M, Suzuki K, Takehira K. Partial oxidation of methane to synthesis gas over some tibanates based perovskite oxides. *Catal Lett*. 1993;22:307-317.
30. Christensen TS, Primdahl II. Improve syngas production using autothermal reforming. *Hydrocarb Process*. 1994;March:39-46.
31. Adris A, Grace J, Lim C, Elnashaie SSEH. *Fluidized Bed Reaction System for Steam/Hydrocarbon Gas Reforming to Produce Hydrogen*. U.S. Patent No. 5 326 550; 1994.
32. Adris AM, Lim CJ, Grace JR. The fluidized bed membrane reactor (FBMR) system: A pilot scale experimental study. *Chem Eng Sci*. 1994;49:5833.
33. Adris AM, Lim CJ, Grace JR. The fluidized-bed membrane reactor for steam methane reforming: Model verification and parametric study. *Chem Eng Sci*. 1997;52:1609.
34. Adris A, Grace J, Lim C, Elnashaie SSEH. *Fluidized Bed Reaction System for Steam/Hydrocarbon Gas Reforming to Produce Hydrogen*. Canadian Patent No. 2 081 70; 2002.
35. Prasad P, Elnashaie SSEH. Novel circulating fluidized bed membrane reformer for the efficient production of ultraclean fuels from hydrocarbons. *Ind Eng Chem Res*. 2002;41:6518-6527.
36. Verykios XE. Catalytic dry reforming of natural gas for the production of chemicals and hydrogen. *Int J Hydrogen Energy*. 2003;28:1045-1063.
37. El Solh T, Jarosch K, de Lasa HI. Fluidized catalyst for methane reforming. *Appl Catal A: Gen*. 2001;210:315-324.
38. Padro CEG, Putsche V. Survey of the economics of hydrogen technologies. NREL/TP-570-27079, September. Golden, CO: Natural Renewable Energy Laboratory; 1999:2.
39. Elnashaie SSEH, Elshishini SS. *Dynamic Modeling, Bifurcation and Chaotic Behavior of Gas–Solid Catalytic Reactors*. London, UK: Gordon & Breach Science Publishers; 1996.
40. Siminski VJ, Wright FJ, Edelman RB, Economos C, Fortune OF. Research on methods of improving the combustion characteristics of liquid hydrocarbon fuels, AFAPL TR 72-74. Vols. I and II. Wright–Patterson Air Force Base, OH: Air Force Aeropropulsion Laboratory, February; 1972.
41. Jin W, Gu X, Li S, Huang P, Xu N, Shi J. Experimental and simulation study on a catalyst packed tubular dense membrane reactor for partial oxidation of methane to syngas. *Chem Eng Sci*. 2000;55:2617-2625.
42. Rostrup-Nielsen JR. Coking on nickel catalysts for steam reforming of hydrocarbons. *J Catal*. 1974;33:184-201.
43. Snoeck JW, Froment GF, Fowles M. Kinetic study of the carbon

filament formation by methane cracking on a nickel catalyst. *J Catal*. 1997;169:250-262.
44. Tottrup PB. Kinetics of decomposition of carbon monoxide on a supported nickel catalyst. *J Catal*. 1976;42:29-36.
45. Chen CX, Horio M, Kojima T. Numerical simulation of entrained flow coal gasifiers. Part I: Modeling of coal gasification in an entrained flow gasifier. *Chem Eng Sci*. 2000;55:3861-3874.
46. Patience GS, Chaouki J, Berruti F, Wong R. Scaling considerations for circulating fluidized bed risers. *Powder Technol.* 1992;72:31-37.
47. Roy S, Pruden BB, Adris AM, Lim CJ, Grace JR. Fluidized bed steam methane reforming with oxygen input. *Chem Eng Sci*. 1999;54:2095.
48. Shu J, Grandjean BPA, Kaliaguine S. Methane steam reforming in asymmetric Pd- and Pd-Ag/porous SS membrane reactor. *Appl Catal A*. 1994;119:305-325.
49. Tsai CY, Dixon AG, Moser WR, Ma YH. Dense perovskite membrane reactors for partial oxidation of membrane to syngas. *AIChE J*. 1997; 43:2741.
50. Barbieri G, Di Maio FP. Simulation of methane steam reforming process in a catalytic Pd-membrane reactor. *Ind Eng Chem Res.* 1997;36:2121-2127.
51. Grace JR. Fluidized bed hydrodynamics. In: Hetrroni G, ed. *Handbook of Multiphase Systems*. Section 8.1. Washington, DC: Hemisphere; 1982:8-5– 8-64.
52. Ritchie JT, Richardson JT, Luss D. Ceramic membrane reactor for synthesis gas production. *AIChE J*. 2001;47:2092-2100.
53. Kunii D, Levenspiel O. Entrainment of solids from fluidized beds: I. Hold-up of solids in the freeboard, II. Operation of fast fluidized beds. *Powder Technol*. 1990;61:193-206.
54. Kunii D, Levenspiel O. Circulating fluidized-bed reactors. *Chem Eng Sci*. 1997;15:2471-2484.
55. Himmelblau DM. *Applied Nonlinear Programming*. New York, NY: McGraw-Hill; 1972:341.

Manuscript received Mar. 31, 2004, and revision received Sept. 10, 2004.